

Study of neutron-deficient nucleus ^{224}Np and its α decay by particle-number-conserving method in the framework of deformed shell model

Xiao-Tao He,^{1,*} Kun Huang,¹ T. M. Shneidman,² N. V. Antonenko,² Jun Zhang,³ and Hong-qiang You³

¹College of Materials Science and Technology, Nanjing University of Aeronautics and Astronautics, Nanjing 210016, China

²Bogoliubov Laboratory of Theoretical Physics, Joint Institute for Nuclear Research, Dubna 141980, Russia

³College of Physics, Nanjing University of Aeronautics and Astronautics, Nanjing 210016, China

(Dated: April 23, 2025)

The particle-number-conserving (PNC) method in the framework of the deformed shell model (DSM) is employed to study the properties of the newly discovered short-lived neutron-deficient nucleus ^{224}Np and its α -decay. The calculated energy of α -particle lies within 300 keV of the experimental data. This is the first application of the PNC method to the region of neutron-deficient nuclei. This work provides the first attempt to combine the microscopic PNC theory with empirical formulas to study the nuclear α decay. The configurations of ground states are assigned as $\pi 5/2^- [523] \otimes \nu 5/2^+ [633]$ for ^{224}Np , $\pi 1/2^- [530] \otimes \nu 3/2^+ [642]$ for ^{220}Pa , $\pi 3/2^+ [651] \otimes \nu 1/2^- [501]$ for ^{216}Ac , and $\pi 7/2^- [514] \otimes \nu 3/2^- [501]$ for ^{212}Fr . The absence of the $Z = 92$ subshell closure in ^{224}Np is explained by analyzing the proton single-particle levels. Low-lying excited states are predicted for nuclei along the α -decay chain by the PNC method. Based on the PNC predicted α -decay energy and the assigned configurations, the α -decay half-lives are calculated by the empirical formulas, in which the angular momentum taken away by the α particle is taken into account. The angular momentum have an important effect on the α -decay half-life. The errors of the empirical formulas calculation are in two orders of magnitude with the experimental data.

I. INTRODUCTION

Radioactive ion beams have greatly expanded our capabilities in the study of nuclear physics, in particular in the study of the structure and properties of nuclei far from the β stable line. Among these, neutron-deficient nuclei are of special interest due to their unique nuclear structure, which is crucial to understanding fundamental nuclear interactions [1, 2]. The evolution of the shell structure beyond the heaviest known double-magic nucleus ^{208}Pb is of great importance for understanding the stability and structure of superheavy nuclei. In this respect, it is interesting to investigate the shell structure around $Z = 92$. The $Z = 92$ shell gap is predicted in the theoretical calculations [3–7]. This is at variance with large-scale shell model calculations [8]. Experimental results on the α -decay and proton separation energies of ^{223}Np [9] and ^{219}Np [10] show no indication of the shell or subshell closure at $Z = 92$.

New heavy neutron-deficient nuclei have been produced, including $^{214,216,218,219,221}\text{U}$ [11–15], ^{220}Pa [16], and $^{219,220,222-224}\text{Np}$ [9, 10, 17–19]. Physicists have described the neutron-deficient region via different models [20, 21]. They drawn the α -decay systematics for the isotopes near $N = 126$ with $89 \leq Z \leq 93$, which support that the robustness of $N = 126$ shell closure up to the Np isotopes [9, 10]. However, research on the α -decay of the odd-odd nucleus ^{224}Np remains unknown area in theoretical calculations, lacking any microscopic structural insights. Remarkably, it stands as the heaviest nucleus residing on the proton drip-line to date.

For unstable nuclei, especially neutron-deficient nuclei, α -decay is a dominant decay mode and plays a significant role in the identification of new elements or new isotopes [9–19].

α -decay provides information on half-lives, decay energies, spin and parities of ground and excited states, as well as important insight on properties of nuclear interaction and shell effects [22–31]. In the theoretical study, α radioactivity was explained successfully as a typical quantum tunneling effect by Gamow [32] and by Condon and Gurney [33] in 1928. Since then, all kinds of theoretical models and empirical formulas have been proposed [34–49]. It was found that the energy of α -decay plays a crucial role in the description of the decay process. Therefore, investigating the α -decay energy is highly significant in revealing nuclear structure and properties of α -decay.

In this work, based on the deformed shell model (DSM) with pairing treated by a particle-number-conserving (PNC) method, the α -decay energies and the microscopic structure of the low-lying excited and ground-states of the nuclei in the α -decay chain of ^{224}Np are studied. This is the first application of the PNC method to the region of neutron-deficient nuclei and to provide a microscopic description of the nuclear α decay. Using the PNC results of the α -decay energies and angular momentum, the half-lives of nuclei along the ^{224}Np α -decay chain are studied by the empirical approaches of Refs. [24, 28, 50].

This article is organized as follows. In Section II A, we present the theoretical framework of the PNC method. The method of calculation of α -decay half-lives presented in Section II B. The calculation details and discussion are given in Section III. Section IV is a summary.

II. THEORETICAL FRAMEWORK

A. PNC method

The detailed description of PNC method can be found in Refs. [51–53]. Here we give a brief introduction of the re-

* hext@nuaa.edu.cn

lated formalism. The deformed shell model Hamiltonian with monopole- and quadrupole- pairing is

$$H_{\text{DSM}} = H_{\text{Nil}} + H_{\text{P}}(0) + H_{\text{P}}(2), \quad (1)$$

$H_{\text{Nil}} = \sum h_{\text{Nil}}$ is the Nilsson Hamiltonian with

$$\begin{aligned} h_{\text{Nil}} = & \frac{1}{2} \hbar \omega_0 (\varepsilon_2, \varepsilon_4, \varepsilon_6) \left[-\nabla_\rho^2 + \frac{1}{3} \varepsilon_2 \left(\frac{2\partial^2}{\partial \xi^2} - \frac{\partial^2}{\partial \xi^2} - \frac{\partial^2}{\partial \eta^2} \right) \right. \\ & + \rho^2 - \frac{2}{3} \varepsilon_2 \rho^2 P_2(\cos \theta_t) + 2\varepsilon_4 \rho^2 P_4(\cos \theta_t) \\ & \left. + 2\varepsilon_6 \rho^2 P_6(\cos \theta_t) \right] - 2\kappa \hbar \omega_0 \left[\vec{l}_t \cdot \vec{s} - \mu (\vec{l}_t^2 - \langle \vec{l}_t^2 \rangle_N) \right]. \end{aligned} \quad (2)$$

where ε_2 , ε_4 and ε_6 are the quadrupole, hexadecapole and high-order deformation parameters, respectively, and the subscript t means that the single-particle Hamiltonian h_{Nil} is written in the stretched coordinates (ξ, η, ζ) , and $\rho^2 = \xi^2 + \eta^2 + \zeta^2$ [54]. $H_{\text{P}}(0)$ and $H_{\text{P}}(2)$ are the monopole- and quadrupole-pairing correlations, respectively.

The H_{DSM} is diagonalized in a sufficiently large many-particle configuration (MPC) space, which is constructed by including the configurations with energy $E_i \leq E_0 + E_c$, where E_0 is the energy of the lowest configuration and E_c is the cutoff energy. The eigenstate of H_{DSM} reads

$$|\psi\rangle = \sum_i C_i |i\rangle, \quad C_i \text{ is real.} \quad (3)$$

$|i\rangle$ is a configuration of the many-particle system. For two unpaired single particles in an odd-odd nucleus with the seniority $\nu = 2$, each $|i\rangle$ in Eq. (3) has the form

$$\begin{aligned} |i\rangle = & |\sigma_1 \sigma_2 \mu_1 \bar{\mu}_1 \cdots \mu_k \bar{\mu}_k\rangle \\ = & b_{\sigma_1}^\dagger b_{\sigma_2}^\dagger b_{\mu_1}^\dagger b_{\bar{\mu}_1}^\dagger \cdots b_{\mu_k}^\dagger b_{\bar{\mu}_k}^\dagger |0\rangle, \quad (\sigma \neq \mu), \end{aligned} \quad (4)$$

where σ_1, σ_2 are the two blocked single-particle states. The angular momentum projection along the nuclear symmetry z axis is $K = |\Omega_{\sigma_1} \pm \Omega_{\sigma_2}|$, and the parity is $\pi = (-)^{N_{\sigma_1} + N_{\sigma_2}}$. The configuration of higher-seniority $\nu > 2$ states is constructed similarly, and the diagonalization remains the same. The blocking effects are considered simultaneously. The state energy E_i for each many-particle configuration $|i\rangle$ is

$$E_i = \sum_{\mu_i (\text{occupied})} \varepsilon_{\mu_i},$$

with ε_{μ_i} is the energy of the occupied Nilsson state. The α particle energy is obtained as

$$E_\alpha = (E_p^{\text{P}} + E_p^{\text{N}}) - (E_d^{\text{P}} + E_d^{\text{N}}), \quad (5)$$

where the superscript P and N denote the state energies for proton and neutron, respectively, and the subscript p and d represent the parent and daughter nuclei, respectively.

B. Empirical formulas for α -decay half-lives

The Royer formula [55] is expressed as

$$\log_{10} T_{1/2} = a + bA^{1/6} \sqrt{Z} + c \frac{Z}{\sqrt{Q_\alpha}}, \quad (6)$$

where A , Z , and Q_α represent the mass number, the proton number, and the α -decay energy, respectively, while a , b , c , are the adjustable parameters. The Royer formula of Eq. (6) describes the favored α decay well, but when extended to the unfavored α decay, large deviations occur between the calculated α decay half-lives and the experimental data due to the effect of the centrifugal potential. The centrifugal potential leads to a higher total barrier, smaller penetration probability of the barrier, and thus to a longer half-life with respect to the α -decay. Therefore, for unfavored α decay, the centrifugal potential plays an important role and cannot be neglected. Based on the original Royer formulas [55], Deng *et al.* develop the new formula [24], where the effect of angular momentum is considered, which can be expressed as

$$\log_{10} T_{1/2} = a + bA^{1/6} \sqrt{Z} + c \frac{Z}{\sqrt{Q_\alpha}} + dl(l+1) + h. \quad (7)$$

Here, the fourth term represents the contribution of the centrifugal potential. The angular momentum carried away by the α -particle is denoted as l . The fifth term represents the blocking effect of unpaired nucleons. For odd-odd nuclei, $a = -26.8125$, $b = -1.1255$, $c = 1.6057$, $d = 0.0513$, $h = 0.7486$ are adopted.

There are still other formulas developing from the Geiger-Nuttall law [28]. It can be expressed as

$$\log_{10} T_{1/2} = a \sqrt{\mu} \frac{Z_1 Z_2}{\sqrt{Q_\alpha}} + b \sqrt{\mu Z_1 Z_2} + c, \quad (8)$$

where Z_1 and Z_2 are the atomic number of daughter and cluster nuclei, respectively. $a = 0.43464$, $b = -1.44876$, and $c = -16.65020$ are free parameter coefficient sets obtained by least square fitting to both α -decay and cluster radioactivity data. μ is the reduced mass.

Based on Eq. (8), an improved formula by including the centrifugal potential and the isospin $I = (N - Z)/A$ correlated term proposed in Ref. [50] as

$$\begin{aligned} \log_{10} T_{1/2} = & a \sqrt{\mu} \frac{Z_1 Z_2}{\sqrt{Q_\alpha}} + b \sqrt{\mu Z_1 Z_2} + c \\ & + dI + eI^2 + f[l(l+1)], \end{aligned} \quad (9)$$

where $a = 0.43323$, $b = -1.40527$, $c = -17.13866$, $d = -7.66291$, $e = 22.26925$ and $f = 0.06902$ are the free parameters obtained by least square fitting to the α -decay data. The angular momentum (l) can be calculated by the following equation,

$$l_{\min} = \begin{cases} \Delta_j & \text{for even } \Delta_j \text{ and } \pi_p = \pi_d, \\ \Delta_j + 1 & \text{for even } \Delta_j \text{ and } \pi_p \neq \pi_d, \\ \Delta_j & \text{for odd } \Delta_j \text{ and } \pi_p \neq \pi_d, \\ \Delta_j + 1 & \text{for odd } \Delta_j \text{ and } \pi_p = \pi_d, \end{cases} \quad (10)$$

where $\Delta_j = |j_p - j_d|$, with j_p, π_p, j_d, π_d are the spin and parity values of the parent and daughter nuclei, respectively.

III. RESULTS AND DISCUSSIONS

A. Parameters

The values of Nilsson parameters (κ, μ) in Eq. (2) are taken from the Lund systematics [54]. The deformations $\varepsilon_2, \varepsilon_4$, and ε_6 are input parameters in the PNC calculations. The values used in the present calculations are listed in the Table I, where ε_2 and ε_4 are larger than the deformation parameters from Ref. [56]. In the present calculations, what used to fit the α -decay energy is taken from Refs. [17, 19], and the high-order axial deformation ε_6 is included due to its important effect on the deformed shell gaps and the further influence on the multiparticle excitation energy.

TABLE I. Deformation parameters $\varepsilon_2, \varepsilon_4$, and ε_6 used in the present calculations for ^{224}Np , ^{220}Pa , ^{216}Ac , and ^{212}Fr .

nuclei	^{224}Np	^{220}Pa	^{216}Ac	^{212}Fr
ε_2	0.118	0.144	0.139	-0.169
ε_4	-0.021	-0.018	-0.030	-0.027
ε_6	0.004	0.004	-0.038	-0.010

The effective pairing strengths G_0, G_2 can be determined by the odd-even differences in nuclear binding energy in principle. These values are linked with the dimensions of the truncated many-particles configuration space. In the present calculations, the MPC spaces for all the nuclei involved are constructed in the proton $N = 4, 5, 6$ and neutron $N = 5, 6$ shells. For both of the protons and neutrons, the dimensions of MPC space are about 1300. For all nuclides except ^{224}Np , the effective monopole- and quadrupole- pairing strengths are $G_0 = 0.2$ MeV, $G_2 = 0.02$ MeV, respectively, while for ^{224}Np , $G_0 = 0.23$ MeV, $G_2 = 0.02$ MeV. The PNC calculations remain stable regardless of the dimension of the MPC space, which has been investigated in Ref. [57].

B. Single particle levels

The single-particle levels are of importance for determining the low-lying multiparticle states. In the current calculations, Nilsson states are computed for the valence single-particle space including proton $N = 4 - 6$ and neutron $N = 5 - 6$ major shells.

Figure 1 shows the single particle levels near the Fermi surface of nuclei along the α -decay chain. The levels are denoted by blue lines with positive parity and red lines with negative parity. Each level is denoted by the quantum numbers $[Nn_z\Lambda]\Omega$. Based on such sequences of single particle levels, the experimental ground state and low-lying excited states can be reproduced well for the neighbor odd-A nuclei, such as the proton ground states in $^{222,223}\text{Np}$ [9, 19], and $^{230,234}\text{Pa}$ [58, 59] and neutron ground states in ^{223}U , ^{217}Th , and ^{213}Ra [60, 61].

For protons, the Fermi surface changes from $\pi 5/2^- [523]$ in ^{224}Np , to $\pi 1/2^- [530]$ in ^{220}Pa , and $\pi 3/2^+ [651]$ in ^{216}Ac . The proton $\pi 5/2^- [523]$ level stems from $h_{9/2}$ orbital and $\pi 1/2^- [530]$ and $\pi 3/2^+ [651]$ levels stem from $i_{13/2}$ orbital. The deformed proton shell at $Z = 92$ is shown for ^{220}Pa and ^{216}Ac while is absent for ^{224}Np and ^{212}Fr in Fig. 1. The results of absence of $Z = 92$ shell gap in ^{224}Np is consistent with Ref. [9], where the same trend is observed for $Z < 92$, providing no sign of the subshell closure at $Z = 92$ from S_p (the single proton separation energies) and δ_p (separation energy difference).

The neutron deformed shell gap at $N = 130$ is shown in ^{224}Np and ^{220}Pa while it disappears in ^{216}Ac . The neutron Fermi surface locates at $N = 126$ neutron shell for ^{212}Fr . Its deformation is quite different from others, changes from prolate to oblate (see the quadrupole deformation parameters in Table I). Therefore, the single-particle level structure differs considerably from these for other nuclei along the α -decay chain.

C. Occupation probability and configuration assignment

The configuration of each multi-particle state is explicitly determined through the wave function. Once the wave function is obtained by Eq. (3), the state configuration can be determined by the occupation probability n_μ ,

$$n_\mu = \sum_i |C_i|^2 P_{i\mu}, \quad C_i \text{ is real}, \quad (11)$$

where $P_{i\mu} = 1$ represents the state $|\mu\rangle$ is occupied and $P_{i\mu} = 0$ otherwise. The total particle number $N = \sum_\mu n_\mu$.

Figure 2 shows the occupation probability n_μ of each proton(top) and neutron(bottom) orbitals μ near the Fermi surface at $\hbar\omega=0$ for ground states in ^{224}Np , ^{220}Pa , ^{216}Ac , and ^{212}Fr , where μ is double degenerate. An orbital is fully occupied at $n_\mu \approx 2$, and blocked at $n_\mu \approx 1$. The occupation probability of Nilsson levels far below ($n_\mu \approx 2$) and far above ($n_\mu \approx 0$) the Fermi surface are not presented.

For ^{224}Np , the blocked orbitals are $\pi 5/2^- [523]$ and $\nu 5/2^+ [633]$ with the values of n_μ of the $\nu 5/2^+ [633]$ orbital and the $\pi 5/2^- [523]$ orbital are both ≈ 1 . Meanwhile, due to the pairing correlation, others orbitals are partially occupied. In Ref. [58], $\pi 1/2^- [530]$ is suggested as the configuration of the ground-state of odd-even Pa isotopes, which is confirmed in the present calculations. From Fig. 2, the configuration of the ground-state for ^{220}Pa can be assigned as $\pi 1/2^- [530] \otimes \nu 3/2^+ [642]$. The ground state configurations of other nuclei can be determined in the same way that is $\pi 3/2^+ [651] \otimes \nu 1/2^- [501]$ for ^{216}Ac , and $\pi 7/2^- [514] \otimes \nu 3/2^- [501]$ for ^{212}Fr , respectively.

Low-lying excitation states are predicted by the PNC calculations. Although due to the configuration mixing, the occupation probability is not as pure as that for the ground state with $n_\mu \approx 1$, excitation state configuration can still be determined by the dominant component in their wave function. The excitation energy together with the configuration of the low-lying state for the nuclei along the α -decay chain is shown in Fig. 3.

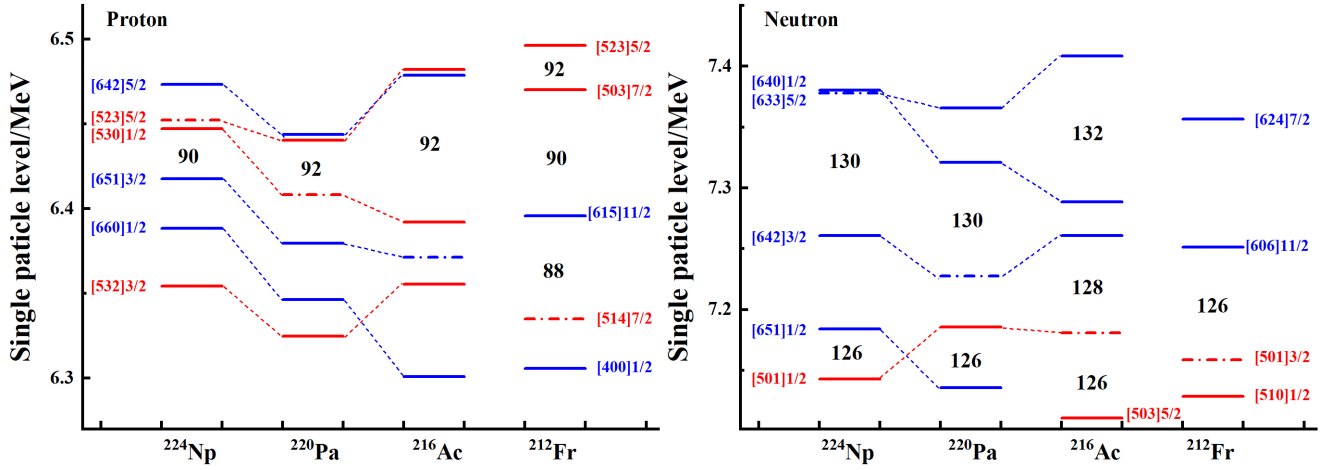


FIG. 1. Single particle levels near the Fermi surface of the nuclei along the α -decay chain of ^{224}Np for protons (left) and neutrons (right). The positive- (negative-) parity levels are denoted by blue (red) lines, and the Fermi surfaces are denoted by dot-dashed lines. The dotted lines are used to guide the eye.

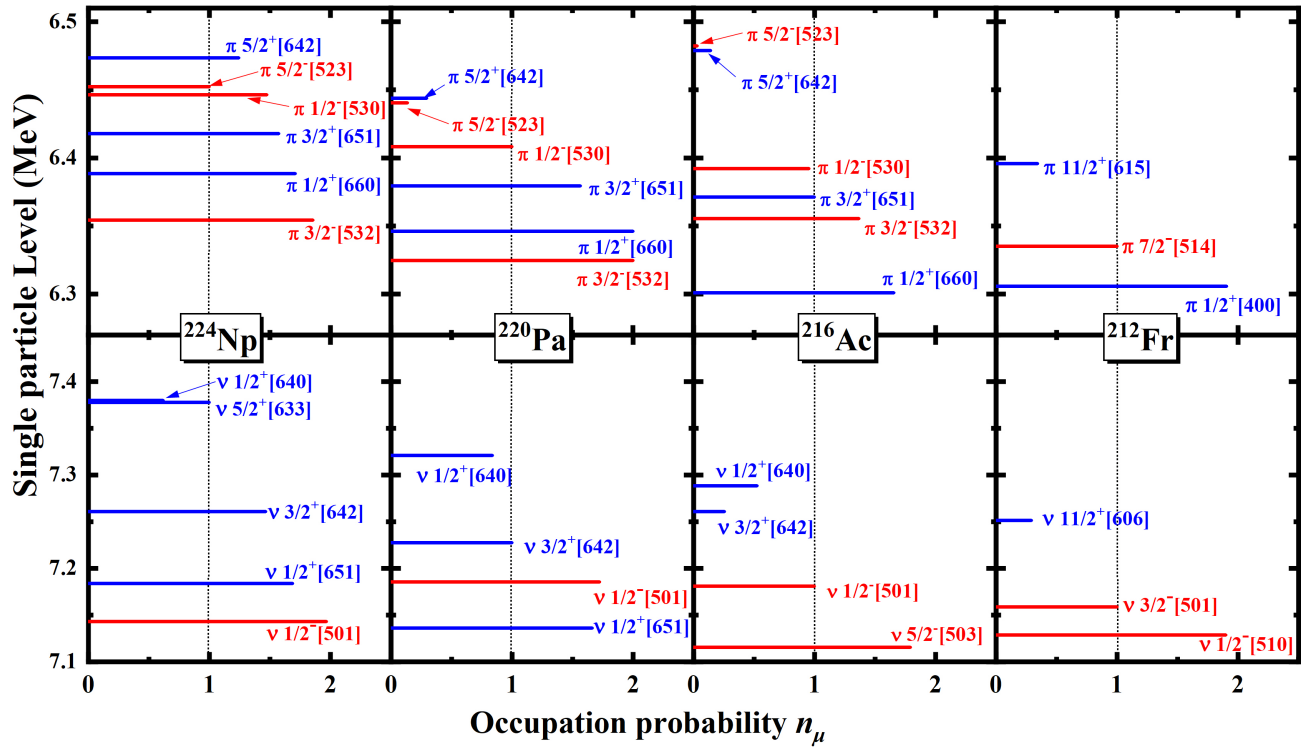


FIG. 2. The occupation probability n_μ of each proton (top) and neutron (bottom) orbitals μ near the Fermi surface for the ground states in ^{224}Np , ^{220}Pa , ^{216}Ac , and ^{212}Fr . The Nilsson levels far below ($n_\mu \approx 2$) and far above ($n_\mu \approx 0$) the Fermi surface are not shown. Positive- (negative-) parity orbitals are denoted by blue (red) lines. The vertical dashed lines are used to guide eye to find the blocked orbitals with $n_\mu = 1$.

D. α -decay properties by PNC-DSM and empirical method

Figure 3 illustrates the comparison between experimental and theoretical α particle energies (E_α), as well as the configurations of ground and low-lying excited states. The thick line represents the ground state, while the thin line denotes the low-

lying excited state. The theoretically determined configurations are on the left of the energy levels, with the excitation energy above the energy levels. We reproduce the experimentally measured α -decay chain well with $\text{Max}|E_\alpha^{\text{cal}} - E_\alpha^{\text{exp}}| < 300$ keV. Based on the configurations assigned by the PNC method, the minimum angular momentum l_{\min} taken away by the α -particle can be obtained by using Eq. (10).

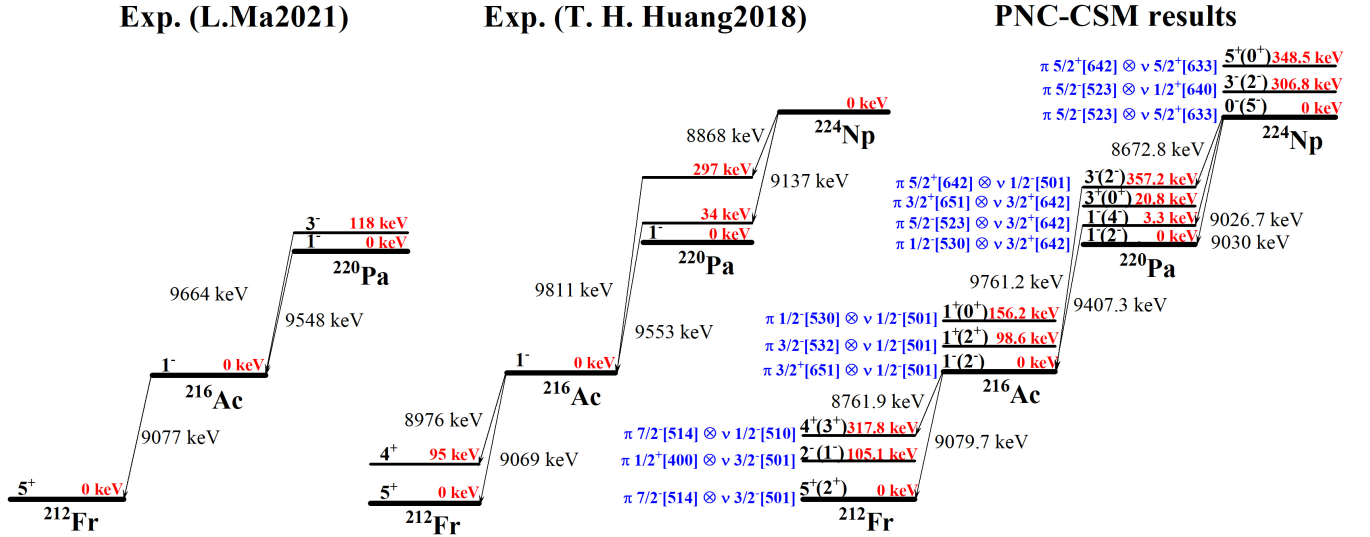


FIG. 3. The comparison of the α particle energy (E_α) and configurations of nuclei in the α -decay chain between experimental (Refs. [16, 17]) and theoretical (PNC) results. The configurations of the theoretical calculation are on the left of the energy levels. The thick and thin lines represent the ground and low-lying excited states, respectively. The K^π values of excited states favored by the GM rules [62] are unbracketed.

The α -decay half-lives are calculated using the empirical formulas Eq. (7), Eq. (8), and Eq. (9). The results are listed in the Table II, where the first column is the configurations of the ground and low-lying excited states obtained by PNC calculation. The second and third columns show the experimental and calculated α -decay energies (Q_α). The fourth column is the minimum angular momentum. The following three columns display the α -decay half-lives calculated by these three different formulas. Subsequently, the available experimental α -decay half-lives are listed in the last column. The data for α -decay half-lives in experiments are taken from Refs. [16, 17]. The deviation between the experimental data and theoretical results lies within two orders of magnitude.

In the PNC calculation, the ground state of ^{224}Np is assigned as $\pi 5/2^- [523] \otimes \nu 5/2^+ [633]$. The configuration of 0^- is adopted, which is favored by the Gallagher-Moszkowski (GM) rules [62]. If the ground state of ^{224}Np is adopted as 5^- , in the decay path from the ground state with $\pi 5/2^- [523] \otimes \nu 5/2^+ [633]$ in ^{224}Np to the excited state of 1^- in ^{220}Pa , the calculated minimum angular momentum l_{min} will be 4. Instead of -3.25 and -3.41 with $l_{min} = 2$ by Eq. (7) and (9), respectively, the calculated α -decay half-lives would be -2.02 and -1.75, which far from the experimental result $38\mu s$ ($\log_{10} T_{1/2} = -4.42$) [17]. The angular momentum taken away by the α particle is important. Two calculated low-lying excited states with energy of 306.8 keV and 348.5 keV is assigned as 5^+ ($\pi 5/2^+ [642] \otimes \nu 5/2^+ [633]$) and 3^- ($\pi 5/2^- [523] \otimes \nu 1/2^+ [640]$), respectively.

For ^{220}Pa , its ground state is established as 1^- , which is consistent with the experimental assignment. In the experiment of Ref. [17], ^{220}Pa exhibits two excited state with energy of 34 keV and 297 keV, respectively, without the detailed configuration information. In the later experimental research [16], an

excited state of 3^- with 118 keV was observed. The PNC calculations reveal that the first excited state has a configuration of $\pi 5/2^- [523] \otimes \nu 3/2^+ [642]$ with excitation energy of 3.3 keV, and a higher excited 3^- state of $\pi 5/2^+ [642] \otimes \nu 1/2^- [501]$ with energy of 357.2 keV is predicted. When the excited state 1^- undergoes favored α -decay to the ground state (1^-) of ^{216}Ac , the calculated results are -5.24, -5.42, and -5.58, which are compared with the value of -6.51 in Ref. [17] in Table II. For unfavored α -decay of the excited state (3^-) to the ground state (1^-) of ^{216}Ac , the results -5.79, -6.33, and -6.07 compared with the value of -6.63 in Ref. [16] in Table II. There are three low-lying excited states, which are not shown in Fig. 3 and Table II. That are $\pi 1/2^- [530] \otimes \nu 1/2^+ [501]$ (25.1 keV), $\pi 5/2^- [523] \otimes \nu 1/2^+ [501]$ (335.4 keV), and $\pi 3/2^+ [651] \otimes \nu 1/2^+ [501]$ (352.9 keV) in ^{220}Pa between 3^+ (20.8 keV) and 3^- (357.2 keV).

The experimental observed 1^- ground state in ^{216}Ac is assigned as $\pi 3/2^+ [651] \otimes \nu 1/2^- [501]$ configuration in the PNC calculations, and two low-lying excited states are predicted at 98.6 keV and 156.2 keV with the configurations of $\pi 3/2^- [532] \otimes \nu 1/2^- [501]$ and $\pi 1/2^- [530] \otimes \nu 1/2^- [501]$, respectively. For ^{212}Fr , the 5^+ state is observed in Refs. [16, 17]. Its configuration is assigned as $\pi 7/2^- [514] \otimes \nu 3/2^- [501]$ in the present calculation. The 4^+ excited state is assigned as $\pi 7/2^- [514] \otimes \nu 1/2^- [510]$ with higher energy of 317.8 keV. When the excited state (1^-) of ^{216}Ac undergoes unfavored α -decay to the ground state (5^+) of ^{212}Fr , the calculated α -decay half-lives are -3.55, -5.25, -3.35. In this case, the angular momentum taken away by the α particle is as large as 5, which leads to an important effect on the α -decay half-life. The results by including the centrifugal terms [Eqs. (7) and (9)] reproduce the experimental better when compared with the value of -3.46 in Ref. [16] in Table II.

IV. SUMMARY

In this work, ^{224}Np and its α -decay are investigated by using the particle-number-conserving method in the framework of the deformed shell model and the empirical formulas. The theoretical results of the α -decay energy and half-lives for the odd-odd nucleus ^{224}Np and its decay chain can reproduce well of the experimental data. The calculated energy of α -particle lies within 300 keV of the experimental data. The Nilsson single-particle levels show the absence of the $Z = 92$ subshell for ^{224}Np . By analyzing the wave function of the deformed shell model Hamiltonian, the configurations are assigned to the experimentally observed ground-state and low-lying excited states. Moreover, more excited states are predicted with the detailed informations of state energy and the configurations by

the PNC-DSM.

Based on the calculated α -decay energy and the assigned configuration of the PNC-DSM, three kinds of the empirical formulas are used to calculate the α -decay half-lives. The theoretical results lie in two orders of magnitude errors with comparison of the experimental data. The angular momentum taken away by the α particles is important, especially for the unfavored decay with large angular momentum changing.

ACKNOWLEDGEMENT

This work is supported by the National Key R&D Program of China (Contract Nos. 2024YFE0109804 and 2023YFA1606503), the National Natural Science Foundation of China (Grant No. 12475121) and the China Scholarship Council (Grant No. EWXM2311280008).

TABLE II: Calculated α -decay half-lives along the decay chains of ^{224}Np by the empirical formulas based on the PNC calculated α -decay energy and configurations. The experimental data are from the Refs. [16, 17].

Configuration	Q_α/keV		l_{min}	$\lg T_{1/2}$			
	Exp.	Cal.		Eq. (7)	Eq. (8)	Eq. (9)	Exp.
$^{224}\text{Np} \longrightarrow ^{220}\text{Pa}$							
$\pi 5/2^+ [642] \otimes \nu 5/2^+ [633] \rightarrow \pi 5/2^+ [642] \otimes \nu 1/2^- [501]$		9185.3	3	-2.92	-3.66	-2.98	
$\pi 5/2^+ [642] \otimes \nu 5/2^+ [633] \rightarrow \pi 3/2^+ [651] \otimes \nu 3/2^+ [642]$		9527.8	2	-4.13	-4.59	-4.33	
$\pi 5/2^+ [642] \otimes \nu 5/2^+ [633] \rightarrow \pi 5/2^- [523] \otimes \nu 3/2^+ [642]$		9545.7	5	-2.94	-4.64	-2.72	
$\pi 5/2^+ [642] \otimes \nu 5/2^+ [633] \rightarrow \pi 1/2^- [530] \otimes \nu 3/2^+ [642]$		9549.0	5	-2.95	-4.65	-2.73	
$\pi 5/2^- [523] \otimes \nu 1/2^+ [640] \rightarrow \pi 5/2^+ [642] \otimes \nu 1/2^- [501]$		9142.9	0	-3.43	-3.54	-3.69	
$\pi 5/2^- [523] \otimes \nu 1/2^+ [640] \rightarrow \pi 3/2^+ [651] \otimes \nu 3/2^+ [642]$		9485.4	1	-4.22	-4.48	-4.49	
$\pi 5/2^- [523] \otimes \nu 1/2^+ [640] \rightarrow \pi 5/2^- [523] \otimes \nu 3/2^+ [642]$		9503.2	2	-4.06	-4.53	-4.26	
$\pi 5/2^- [523] \otimes \nu 1/2^+ [640] \rightarrow \pi 1/2^- [530] \otimes \nu 3/2^+ [642]$		9506.6	2	-4.07	-4.54	-4.27	
$\pi 5/2^- [523] \otimes \nu 5/2^+ [633] \rightarrow \pi 5/2^+ [642] \otimes \nu 1/2^- [501]$	9029.2 [17]	8830.5	4	-1.53	-2.63	-1.40	
$\pi 5/2^- [523] \otimes \nu 5/2^+ [633] \rightarrow \pi 3/2^+ [651] \otimes \nu 3/2^+ [642]$		9173.0	3	-2.89	-3.62	-2.95	
$\pi 5/2^- [523] \otimes \nu 5/2^+ [633] \rightarrow \pi 5/2^- [523] \otimes \nu 3/2^+ [642]$	9303.1 [17]	9190.8	2	-3.25	-3.67	-3.41	-4.42 [17]
$\pi 5/2^- [523] \otimes \nu 5/2^+ [633] \rightarrow \pi 1/2^- [530] \otimes \nu 3/2^+ [642]$		9194.2	2	-3.26	-3.68	-3.42	
$^{220}\text{Pa} \longrightarrow ^{216}\text{Ac}$							
$\pi 5/2^+ [642] \otimes \nu 1/2^- [501] \rightarrow \pi 1/2^- [530] \otimes \nu 1/2^- [501]$		9782.9	3	-5.11	-5.94	-5.26	
$\pi 5/2^+ [642] \otimes \nu 1/2^- [501] \rightarrow \pi 3/2^- [532] \otimes \nu 1/2^- [501]$		9841.5	3	-5.25	-6.08	-5.41	
$\pi 5/2^+ [642] \otimes \nu 1/2^- [501] \rightarrow \pi 3/2^+ [651] \otimes \nu 1/2^- [501]$	9843.0 [16]	9942.0	2	-5.79	-6.33	-6.07	-6.63 [16]
	9992.7 [17]						-7.16 [17]
$\pi 3/2^+ [651] \otimes \nu 3/2^+ [642] \rightarrow \pi 1/2^- [530] \otimes \nu 1/2^- [501]$		9440.2	2	-4.58	-5.05	-4.80	
$\pi 3/2^+ [651] \otimes \nu 3/2^+ [642] \rightarrow \pi 3/2^- [532] \otimes \nu 1/2^- [501]$		9498.9	2	-4.73	-5.21	-4.95	
$\pi 3/2^+ [651] \otimes \nu 3/2^+ [642] \rightarrow \pi 3/2^+ [651] \otimes \nu 1/2^- [501]$		9599.3	3	-4.67	-5.47	-4.80	
$\pi 5/2^- [523] \otimes \nu 3/2^+ [642] \rightarrow \pi 1/2^- [530] \otimes \nu 1/2^- [501]$		9422.4	1	-4.74	-5.01	-5.03	
$\pi 5/2^- [523] \otimes \nu 3/2^+ [642] \rightarrow \pi 3/2^- [532] \otimes \nu 1/2^- [501]$		9481.1	1	-4.89	-5.16	-5.18	
$\pi 5/2^- [523] \otimes \nu 3/2^+ [642] \rightarrow \pi 3/2^+ [651] \otimes \nu 1/2^- [501]$	9729.9 [17]	9581.5	0	-5.24	-5.42	-5.58	-6.51 [17]
$\pi 1/2^- [530] \otimes \nu 3/2^+ [642] \rightarrow \pi 1/2^- [530] \otimes \nu 1/2^- [501]$		9419.1	1	-4.73	-5.00	-5.02	

TABLE II: Calculated α -decay half-lives along the decay chains of ^{224}Np by the empirical formulas based on the PNC calculated α -decay energies and configurations. The experimental data are from the Refs. [16, 17].

Configuration	Q_α/keV		l_{min}	$\lg T_{1/2}$			
	Exp.	Cal.		Eq. (7)	Eq. (8)	Eq. (9)	Exp.
$\pi 1/2^- [530] \otimes \nu 3/2^+ [642] \rightarrow \pi 3/2^- [532] \otimes \nu 1/2^- [501]$		9477.7	1	-4.88	-5.15	-5.17	
$\pi 1/2^- [530] \otimes \nu 3/2^+ [642] \rightarrow \pi 3/2^+ [651] \otimes \nu 1/2^- [501]$	9724.8 [16]	9578.1	0	-5.23	-5.41	-5.57	-6.13 [16]
$^{216}\text{Ac} \rightarrow ^{212}\text{Fr}$							
$\pi 1/2^- [530] \otimes \nu 1/2^- [501] \rightarrow \pi 7/2^- [514] \otimes \nu 1/2^- [510]$		9806.4	4	-3.64	-4.80	-3.60	
$\pi 1/2^- [530] \otimes \nu 1/2^- [501] \rightarrow \pi 1/2^+ [400] \otimes \nu 3/2^- [501]$		9303.1	1	-5.12	-5.39	-5.42	
$\pi 1/2^- [530] \otimes \nu 1/2^- [501] \rightarrow \pi 7/2^- [514] \otimes \nu 3/2^- [501]$		9410.2	4	-4.46	-5.67	-4.46	
$\pi 3/2^- [532] \otimes \nu 1/2^- [501] \rightarrow \pi 7/2^- [514] \otimes \nu 1/2^- [510]$		9027.7	4	-3.48	-4.64	-3.44	
$\pi 3/2^- [532] \otimes \nu 1/2^- [501] \rightarrow \pi 1/2^+ [400] \otimes \nu 3/2^- [501]$		9244.4	1	-4.97	-5.23	-5.26	
$\pi 3/2^- [532] \otimes \nu 1/2^- [501] \rightarrow \pi 7/2^- [514] \otimes \nu 3/2^- [501]$		9351.5	4	-4.31	-5.51	-4.30	
$\pi 3/2^+ [651] \otimes \nu 1/2^- [501] \rightarrow \pi 7/2^- [514] \otimes \nu 1/2^- [510]$	9145.4 [17]	8927.2	3	-3.63	-4.36	-3.71	
$\pi 3/2^+ [651] \otimes \nu 1/2^- [501] \rightarrow \pi 1/2^+ [400] \otimes \nu 3/2^- [501]$		9143.9	2	-4.51	-4.96	-4.72	
$\pi 3/2^+ [651] \otimes \nu 1/2^- [501] \rightarrow \pi 7/2^- [514] \otimes \nu 3/2^- [501]$	9240.1 [17]	9251.0	5	-3.55	-5.25	-3.35	
	9248.3 [16]						-3.46 [16]

- [1] C. Qi, *Reviews in Physics* **1**, 77 (2016).
- [2] N. Benhamouda, M. Oudih, N. Allal, and M. Fellah, *Acta Physica Hungarica New Series-Heavy Ion Physics* **19**, 191 (2004).
- [3] K. Rutz, M. Bender, P. G. Reinhard, J. A. Maruhn, and W. Greiner, *Nuclear Physics A* **634**, 67 (1998).
- [4] L. S. Geng, H. Toki, and J. Meng, *Progress of theoretical physics* **113**, 785 (2005).
- [5] L. S. Geng, J. Meng, T. Hiroshi, W. H. Long, and G. Shen, **23**, 1139 – 1141 (2006), all Open Access, Green Open Access.
- [6] H. Sagawa and G. Colò, *Progress in Particle and Nuclear Physics* **76**, 76 (2014).
- [7] P. Möller, J. Nix, and K.-L. Kratz, *Atomic Data and Nuclear Data Tables* **66**, 131 (1997).
- [8] E. Caurier, M. Rejmund, and H. Grawe, *Physical Review C* **67**, 054310 (2003).
- [9] M. Sun, Z. Liu, T. Huang, W. Zhang, J. Wang, X. Liu, B. Ding, Z. Gan, L. Ma, H. Yang, Z. Zhang, L. Yu, J. Jiang, K. Wang, Y. Wang, M. Liu, Z. Li, J. Li, X. Wang, H. Lu, C. Lin, L. Sun, N. Ma, C. Yuan, W. Zuo, H. Xu, X. Zhou, G. Xiao, C. Qi, and F. Zhang, *Physics Letters B* **771**, 303 (2017).
- [10] H. Yang, L. Ma, Z. Zhang, C. Yang, Z. Gan, M. Zhang, M. Huang, L. Yu, J. Jiang, Y. Tian, Y. Wang, J. Wang, Z. Liu, M. Liu, L. Duan, S. Zhou, Z. Ren, X. Zhou, H. Xu, and G. Xiao, *Physics Letters B* **777**, 212 (2018).
- [11] Z. Zhang, H. Yang, M. Huang, Z. Gan, C. Yuan, C. Qi, A. Andreyev, M. Liu, L. Ma, M. Zhang, *et al.*, *Physical Review Letters* **126**, 152502 (2021).
- [12] L. Ma, Z. Y. Zhang, Z. G. Gan, H. B. Yang, L. Yu, J. Jiang, J. G. Wang, Y. L. Tian, Y. S. Wang, S. Guo, B. Ding, Z. Z. Ren, S. G. Zhou, X. H. Zhou, H. S. Xu, and G. Q. Xiao, *Physical Review C* **91**, 051302 (2015).
- [13] A. Leppänen, J. Uusitalo, M. Leino, S. Eeckhaudt, T. Grahn, P. Greenlees, P. Jones, R. Julin, S. Juutinen, H. Kettunen, *et al.*, *Physical Review C* **75**, 054307 (2007).
- [14] A. Andreyev, D. Bogdanov, V. Chepigin, A. Kabachenko, O. Malyshev, R. Sagaidak, G. Ter-Akopian, M. Veselsky, and A. Yeremin, *Zeitschrift für Physik A Hadrons and Nuclei* **345**, 247 (1993).
- [15] J. Khuyagbaatar, A. Yakushev, C. E. Düllmann, D. Ackermann, L.-L. Andersson, M. Block, H. Brand, D. Cox, J. Even, U. Forsberg, *et al.*, *Physical Review Letters* **115**, 242502 (2015).
- [16] L. Ma, Z. Y. Zhang, H. B. Yang, M. H. Huang, M. M. Zhang, Y. L. Tian, C. L. Yang, Y. S. Wang, Z. Zhao, W. X. Huang, Z. Liu, X. H. Zhou, and Z. G. Gan, *Physical Review C* **104**, 044310 (2021).
- [17] T. H. Huang, W. Q. Zhang, M. D. Sun, Z. Liu, J. G. Wang, X. Y. Liu, B. Ding, Z. G. Gan, L. Ma, H. B. Yang, Z. Y. Zhang, L. Yu, J. Jiang, K. L. Wang, Y. S. Wang, M. L. Liu, Z. H. Li, J. Li, X. Wang, H. Y. Lu, A. H. Feng, C. J. Lin, L. J. Sun, N. R. Ma, D. X. Wang, F. S. Zhang, W. Zuo, X. H. Zhou, H. S. Xu, and G. Q. Xiao, *Physical Review C* **98**, 044302 (2018).
- [18] Z. Zhang, Z. Gan, H. Yang, L. Ma, M. Huang, C. Yang, M. Zhang, Y. Tian, Y. Wang, M. Sun, H. Lu, W. Zhang, H. Zhou, X. Wang, C. Wu, L. Duan, W. Huang, Z. Liu, Z. Ren, S. Zhou, X. Zhou, H. Xu, Y. Tsyganov, A. Voinov, and A. Polyakov, *Physical Review Letters* **122**, 192503 (2019).
- [19] L. Ma, Z. Zhang, Z. Gan, X. Zhou, H. Yang, M. Huang, C. Yang, M. Zhang, Y. Tian, Y. Wang, H. Zhou, X. He, Y. Mao, W. Hua, L. Duan, W. Huang, Z. Liu, X. Xu, Z. Ren, S. Zhou, and H. Xu, *Physical Review Letters* **125**, 032502 (2020).
- [20] G. G. Adamian, N. V. Antonenko, W. Scheid, and A. S. Zubov, *Physical Review C* **78**, 044605 (2008).
- [21] C. He and J. Y. Guo, *Physical Review C* **106**, 064310 (2022).

- [22] W. Yahya, I. Olusola, A. Saeed, and O. Azeez, *Nuclear Physics A* **1018**, 122360 (2022).
- [23] D. T. Akrawy and A. H. Ahmed, *Physical Review C* **100**, 044618 (2019).
- [24] J. G. Deng, H. F. Zhang, and G. Royer, *Physical Review C* **101**, 034307 (2020).
- [25] Y. Ren and Z. Ren, *Physical Review C* **85**, 044608 (2012).
- [26] G. Royer, *Nuclear Physics A* **848**, 279 (2010).
- [27] Z. Ren, C. Xu, and Z. Wang, *Physical Review C* **70**, 034304 (2004).
- [28] D. Ni, Z. Ren, T. Dong, and C. Xu, *Physical Review C* **78**, 044310 (2008).
- [29] G. Saxena, P. K. Sharma, and P. Saxena, *Journal of Physics G: Nuclear and Particle Physics* **48**, 055103 (2021).
- [30] V. Zanganah, D. T. Akrawy, H. Hassanabadi, S. Hosseini, and S. Thakur, *Nuclear Physics A* **997**, 121714 (2020).
- [31] A. Daei-Ataollah, O. N. Ghodsi, and M. Mahdavi, *Physical Review C* **97**, 054621 (2018).
- [32] G. Gamow, *Nature* **122**, 805 (1928).
- [33] R. W. Gurney and E. U. Condon, *Nature* **122**, 439 (1928).
- [34] D. N. Poenaru, R. A. Gherghescu, and W. Greiner, *Physical Review Letters* **107**, 062503 (2011).
- [35] D. N. Poenaru, R. A. Gherghescu, and W. Greiner, *Physical Review C* **85**, 034615 (2012).
- [36] C. Samanta, P. R. Chowdhury, and D. Basu, *Nuclear Physics A* **789**, 142 (2007).
- [37] M. Bhattacharya and G. Gangopadhyay, *Physics Letters B* **651**, 263 (2007).
- [38] D. N. Basu, P. R. Chowdhury, and C. Samanta, *Physical Review C* **72**, 051601 (2005).
- [39] P. R. Chowdhury, C. Samanta, and D. N. Basu, *Physical Review C* **73**, 014612 (2006).
- [40] P. R. Chowdhury, C. Samanta, and D. N. Basu, *Physical Review C* **77**, 044603 (2008).
- [41] X. J. Bao, S. Q. Guo, H. F. Zhang, Y. Z. Xing, J. M. Dong, and J. Q. Li, *Journal of Physics G: Nuclear and Particle Physics* **42**, 085101 (2015).
- [42] H. Zhang, W. Zuo, J. Li, and G. Royer, *Physical Review C* **74**, 017304 (2006).
- [43] C. Xu and Z. Ren, *Nuclear Physics A* **760**, 303 (2005).
- [44] C. Xu and Z. Ren, *Physical Review C* **74**, 014304 (2006).
- [45] B. Buck, A. Merchant, and S. Perez, *Physical Review Letters* **65**, 2975 (1990).
- [46] G. Royer and R. Gherghescu, *Nuclear Physics A* **699**, 479 (2002).
- [47] G. Royer, K. Zbiri, and C. Bonilla, *Nuclear Physics A* **730**, 355 (2004).
- [48] J. M. Dong, H. F. Zhang, and G. Royer, *Physical Review C* **79**, 054330 (2009).
- [49] J. M. Wang, H. F. Zhang, and J. Q. Li, *Journal of Physics G: Nuclear and Particle Physics* **41**, 065102 (2014).
- [50] D. T. Akrawy, H. Hassanabadi, Y. Qian, and K. Santhosh, *Nuclear Physics A* **983**, 310 (2019).
- [51] X. T. He and Y. C. Li, *Physical Review C* **98**, 064314 (2018).
- [52] X. T. He and Y. C. Li, *Physical Review C* **102**, 064328 (2020).
- [53] J. Zhang, X. T. He, Y. C. Li, and H. Q. Zhang, *Physical Review C* **107**, 024305 (2023).
- [54] S. G. Nilsson, C. F. Tsang, A. Sobczewski, Z. Szymański, S. Wycech, C. Gustafson, I.-L. Lamm, P. Möller, and B. Nilsson, *Nuclear Physics A* **131**, 1 (1969).
- [55] G. Royer, *Journal of Physics G: Nuclear and Particle Physics* **26**, 1149 (2000).
- [56] P. Möller, A. J. Sierk, T. Ichikawa, and H. Sagawa, *Atomic Data and Nuclear Data Tables* **109**, 1 (2016).
- [57] S. X. Liu and J. Y. Zeng, *Physical Review C* **66**, 067301 (2002).
- [58] T. Kotthaus, P. Reiter, H. Hess, M. Kalkühler, A. Wendt, A. Wiens, R. Hertenberger, T. Morgan, P. Thierolf, H.-F. Wirth, *et al.*, *Physical Review C* **87**, 044322 (2013).
- [59] Y. Chu and G. Scharff-Goldhaber, *Physical Review C* **17**, 1507 (1978).
- [60] M. Sun, Z. Liu, T. Huang, W. Zhang, A. Andreyev, B. Ding, J. Wang, X. Liu, H. Lu, D. Hou, Z. Gan, L. Ma, H. Yang, Z. Zhang, L. Yu, J. Jiang, K. Wang, Y. Wang, M. Liu, Z. Li, J. Li, X. Wang, A. Feng, C. Lin, L. Sun, N. Ma, W. Zuo, H. Xu, X. Zhou, G. Xiao, C. Qi, and F. Zhang, *Physics Letters B* **800**, 135096 (2020).
- [61] K. Nishio, H. Ikezoe, S. Mitsuoka, and J. Lu, *Physical Review C* **61**, 034309 (2000).
- [62] C. J. Gallagher, *Physical Review* **126**, 1525 (1962).